JACS
JOURNAL OF THE AMERICAN CHEMICAL SOCIETY

COMMUNICATION

pubs.acs.org/JACS

Hydrogen Tunneling Steps in Cyclooxygenase-2 Catalysis

Husain H. Danish, Irina S. Doncheva, and Justine P. Roth*

Department of Chemistry, Johns Hopkins University, 3400 North Charles Street, Baltimore, Maryland 21218, United States

Supporting Information

ABSTRACT: Cyclooxygenases-1 and -2 are tyrosyl radical (Y·)-utilizing hemoproteins responsible for the biosynthesis of lipid-derived autocoids. COX-2, in particular, is a primary mediator of inflammation and believed to be up-regulated in many forms of cancer. Described here are first-of-a-kind studies of COX-2-catalyzed oxidation of the substrate analogue linoleic acid. Very large ($\geq$20) temperature-independent deuterium kinetic isotope effects (KIEs) on the rate constant for enzyme turnover were observed, due to hydrogen atom abstraction from the bisallylic C−H(D) of the fatty acid. The magnitude of the KIE depends on the O_2 concentration, consistent with reversible H/D tunneling mediated by the catalytic Y·. At physiological levels of O_2, retention of the hydrogen initially abstracted by the catalytic tyrosine results in strongly temperature-dependent KIEs on O−H(D) homolysis, also characteristic of nuclear tunneling.

The cyclooxygenases are ~60% homologous hemoproteins expressed by unique genes for the biosynthesis of prostaglandin H_2 from arachidonic acid (AA).[1,2] Whereas cyclooxygenase-1 (COX-1) is present at basal levels in almost every type of cell, cyclooxygenase-2 (COX-2) is induced in response to numerous stimuli, including growth factors and pro-inflammatory cytokines.[3] Recent reports claim that COX-2 is up-regulated in many forms of cancer, where it is believed to make cells resistant to apoptosis.[4,5] The development of new isoform-specific inhibitors (COXibs) that lack cardiotoxic side effects is critical to biomedical research efforts. Reported here is evidence for two hydrogen tunneling steps during the dioxygenase phase of COX catalysis (Scheme 1).[6] The results provide insights essential to understanding enzyme function and possibly the design of new types of COXibs.[1−4]

Of the two kinetic models proposed to describe COX catalysis, the "branched-chain" model is generally favored because it predicts the independent functioning of peroxidase and dioxygenase active sites, which are associated with the heme and tyrosyl radical, respectively. At the center of Scheme 1, the initiating step is oxidation of the conserved tyrosine (Y371 in COX-2) by a "compound I-like" ferryl intermediate formed in the peroxidase cycle. This species and the related reduced forms (shown in red) result from reaction of ferric protoporphyrin IX (Fe^{III}Por) with a hydroperoxide compound (RO_2H or PGG_2 for prostaglandin G_2) followed by the transfer of two reducing equivalents of unknown origin. In enzyme assays, phenol is often used as the sacrificial reductant. The conserved tyrosyl radical, formed as a result of *internal* peroxidase activity, initiates dioxygenase turnover; this involves abstraction of the pro-*S* hydrogen followed by antarafacial attack of O_2 upon the substrate-derived pentadienyl radical. In the case of AA, two 5-exo cyclization steps produce the PGG_2·, which undergoes a final hydrogen transfer. Added reductant may compete with Y371 as the hydrogen atom donor to the terminal peroxyl radical intermediate (as shown in blue), thereby terminating the dioxygenase catalytic cycle. When such reactivity predominates, a "tightly-coupled" model in which one peroxidase turnover is required for every dioxygenase turnover best describes Scheme 1.

Scheme 1. Splicing of Peroxidase and Dioxygenase Activities in One Subunit of the Dimeric Cyclooxygenase

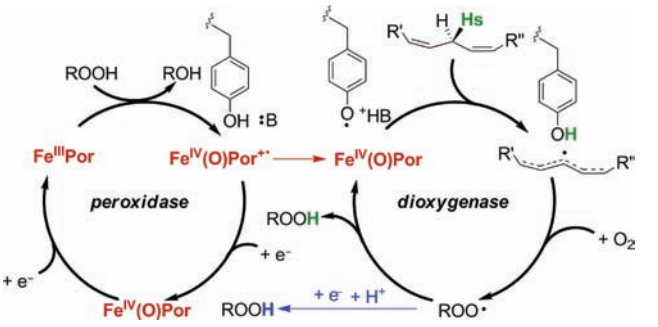

Scheme 2. Major Products of Fatty Acid Oxidation by COX

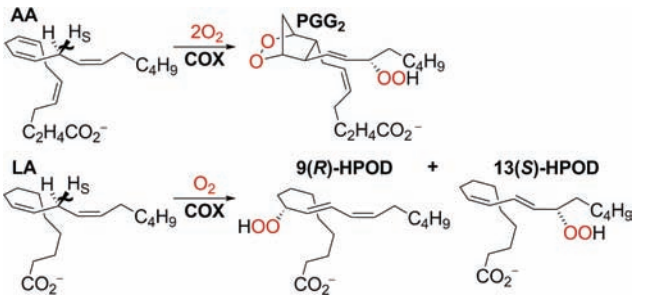

The vast majority of studies have focused on ovine COX-1 isolated from native sources.[7] We have investigated this enzyme's dioxygenase mechanism using steady-state kinetics and ^{18}O kinetic isotope effects (KIEs) to relate AA oxidation to oxidation of the substrate analogue linoleic acid (LA).[8] Because LA has only two double bonds and reacts with one rather than two O_2 equivalents, the (9*R*)- and (13*S*)-hydroperoxyoctadecadienoic

Received: June 27, 2011
Published: September 08, 2011

dx.doi.org/10.1021/ja2059523 | *J. Am. Chem. Soc.* 2011, 133, 15846–15849

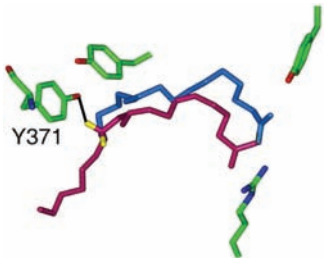

Figure 1. Co^{III}—COX-2 with AA (magenta) and PA (cyan) (PDB entries 3HS5 and 3QH0, respectively) showing hydrogen bonding to the carboxylate termini. A line connects the reactive pro-*S* hydrogen on C(13) of AA (yellow) and Y371.[10,11]

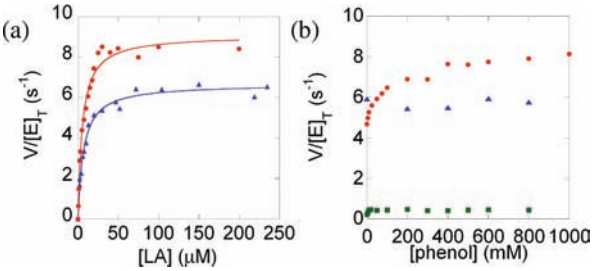

Figure 2. (a) Oxidation of h_{31}-LA by Fe^{III}—COX-2 (●) and Mn^{III}—COX-2 (▲) at saturating levels of O_2, phenol, and 0.44 μM HPOD. (b) Effect of phenol on the above reactions as well as on the oxidation of d_{31}-LA by Fe^{III}—COX-2 (■) at 30 °C.

acids (HPODs) are formed as the primary products[9] in lieu of the bicyclic endoperoxide PGG_2 (Scheme 2).

Crystallographic studies suggest that AA and LA bind similarly to COX-1[10] and COX-2,[11] resulting in the L-shaped conformations depicted above. In Figure 1, AA and the saturated 16-carbon palmitic acid (PA) are superimposed.[11a] These results, along with the structures of AA and LA bound to COX-1,[8,10] suggest that LA should be positioned analogously to AA in COX-2, with the pro-*S* hydrogen at C(11) pointed toward Y371.

Steady-state measurements with Fe^{III}—COX-1 comparing the rates of oxidizing h_{31}- and d_{31}-LA[12] have revealed unexpectedly large deuterium KIEs (>30 at pH 8.0 and 30 °C).[13a] The KIE is increased from ~5 in the absence of phenol to ~38 in solutions containing 0.3 mM phenol. The kinetic behavior is difficult to analyze, however, because added phenol results in competing acceleratory and inhibitory effects.[8,14] The less kinetically complex phenol dependence of Fe^{III}—COX-2 examined here allows two hydrogen tunneling steps to be resolved during the dioxygenase reaction.

His_6-tagged human COX-2 was expressed in baculovirus-infected sf9 insect cells and purified, as described previously,[13b,15] to afford a 150 kD homodimer of >95% purity. The apoprotein was reconstituted with hematin (Sigma) or manganese(III) protoporphyrin IX chloride (Frontier Scientific) and purified, affording Fe^{III}(Por) or Mn^{III}(Por) tightly but noncovalently bound to each subunit.[1,2] In kinetic experiments, the holoprotein could be generated by addition of the prosthetic group to the apoprotein in the presence of O_2 just before initiation with fatty acid. As found previously,[8,16] trace hydroperoxide impurities in the fatty acid preparations were sufficient to sustain a maximum rate of dioxygenase turnover followed by relatively slow enzyme deactivation.

Titrations of apo-COX-2 with substoichiometric equivalents of the prosthetic group revealed the expected half-of-sites reactivity.[13b] This property has been attributed to the formation of a "conformational heterodimer" having only one catalytically active subunit as result of a structural perturbation in the second subunit upon binding of fatty acid to the first.[11b,17] The turnover rate constant (k_{cat}), defined at saturating levels of all substrates, is indistinguishable from that of the isolated holoprotein.[13b] The holoprotein concentration was determined from its electronic absorption spectrum and molar extinction coefficient(s) associated with the Soret band(s) of Fe^{III}(Por) and Mn^{III}(Por).[18] On this basis, a standard assay was developed from the initial rate of O_2 uptake (V) divided by the total holoprotein concentration in 16 mM sodium pyrophosphate (pH 8). The value $V/[E]_T = 15$ s^{-1} at 30 °C for air-saturated solutions containing 50 μM AA and 1 mM phenol was used to calculate the active enzyme concentration in assays using an O_2 electrode (YSI) after incubation at temperatures from 5 to 50 ± 0.2 °C.[8,13b] Unless otherwise specified, measurements were conducted at 30 °C, where Fe^{III}—COX-2 exhibits a k_{cat} for AA that is 2 times larger than k_{cat} for LA. The difference is expected because of the change in fatty acid-to-O_2 stoichiometry shown in Scheme 2. The K_M(AA) value is ~2 times smaller than K_M(LA) = 5.3 ± 1.0 μM. In the limit where K_M approaches K_D, this is consistent with the fatty acids having similar binding affinities. The value $K_M(O_2)$ = 13.0 ± 1.4 μM determined with AA is almost 10 times smaller than $K_M(O_2)$ with LA, elevating $k_{cat}/K_M(O_2)$ significantly.

Although this study focuses upon Fe^{III}—COX-2, Mn^{III}—COX-2 was used in control experiments to test the assumption that Y371· is responsible for the enzyme's dioxygenase activity. Mn^{III}COX-2 exhibits impaired peroxidase reactivity that slows the reaction: Mn^{III}(Por) + RO_2H → [Mn^{V}═O(Por) + ROH] → Mn^{IV}═O-(Por) + Y371· (cf. Scheme 1). However, an optimal rate for dioxygenase turnover, approaching that for Fe^{III}—COX-2, is achieved upon addition of (9*R*)- or (13*S*)-HPOD, independent of the concentration of phenol. At saturating hydroperoxide levels, the Michaelis constants for LA and O_2 are also similar for Mn^{III}—COX-2 and Fe^{III}—COX-2, consistent with Y371· being the active catalyst.

Oxidation of LA by Fe^{III}—COX-2 and Mn^{III}—COX-2 is compared in Figure 2. In experiments with Fe^{III}—COX-2, phenol was present at 2 mM in order to achieve optimal rates.[13b] In contrast, oxidations of h_{31}- and d_{31}-LA by Mn^{III}—COX-2 are unaffected by added phenol (only the former is shown in Figure 2b for clarity), at HPOD saturation. The data under these conditions indicate that the k_{cat} value of 6.7 ± 0.2 s^{-1} for Mn^{III}—COX-2 is somewhat smaller than the k_{cat} value of 9.1 ± 0.4 s^{-1} for Fe^{III}—COX-2, whereas the K_M(LA) value is the same within the limits of error (6.7 ± 1.1 μM). A small difference in k_{cat} has also been observed with AA,[1] raising the possibility that the concentration of Y371· varies. Nevertheless, the $^{D}k_{cat}$ value of 21.0 ± 3.0 for Mn^{III}—COX-2 is indistinguishable from the $^{D}k_{cat}$ value of 22.0 ± 1.0 for Fe^{III}—COX-2. The latter was reproduced using electronic absorption spectroscopy[19] by monitoring the initial rates for formation of the 9- and 13-HPODs, which are converted enzymatically to the corresponding hydroxyoctadecadienoic acids (HODs).[9,13b]

Fe^{III}—COX-1[8] and Fe^{III}—COX-2 exhibit apparent rate constants, $^{ap}k_{cat}/K_M(O_2)$ and $^{ap}k_{cat}/K_M$(LA), that depend on the concentration of the cosubstrate. We have interpreted this observation, together with small tritium KIEs reported earlier,[20] to indicate a reversible reaction wherein the Y· converts the fatty

dx.doi.org/10.1021/ja2059523 |*J. Am. Chem. Soc.* 2011, 133, 15846–15849

Scheme 3. Proposed Dioxygenase Mechanism

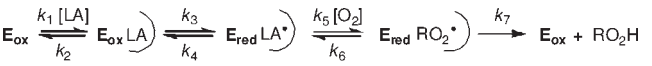

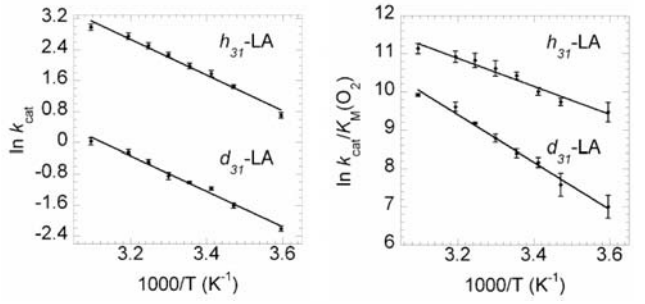

Figure 3. Rate constants for the oxidation of LA (100 μM) by Fe^{III}—COX-2 at variable temperatures and 2.0 mM phenol.[13b]

Table 1. Isotopic Rate Constants and Activation Parameters for LA Oxidation by Fe^{III}—COX-2 between 5 and 50 °C[a]

	KIE(30 °C)[b]	$E_a(D) - E_a(H)$ (kcal mol^{-1}) [b]	A_H/A_D
$^Dk_{cat}$	22.1 ± 1.0 [c]	0.01 ± 0.66	20 ± 14
$^Dk_{cat}/K_M(O_2)$	6.2 ± 1.6	5.0 ± 0.78	0.0014 ± 0.0010

[a] Data were collected under the conditions described in the text. [b] Errors of $\pm 2\sigma_e$ were derived from linear regression analysis of unweighted rate constants. [c] For Mn^{III}—COX-2, $^Dk_{cat}$ = 21.0 ± 3.0.

acid into a delocalized pentadienyl radical prior to interacting with O_2.[8] This is the mechanism shown in Scheme 3, which accounts for the hyperbolic increase in the apparent substrate deuterium KIE in response to increases in the concentration of O_2. Such behavior has also been observed in a fatty acid α-dioxygenase with 15% homology to COX, which utilizes a conserved Y· to oxidize fatty acids to (2*R*)-hydroperoxide compounds.[21]

The hyperbolic increase in the apparent deuterium KIEs to $^Dk_{cat} \geq 20$ for Fe^{III}— and Mn^{III}—COX-2[13b] indicates that C—H(D) homolysis ranges from reversible at low O_2 concentrations to irreversible as the O_2 concentration reaches the saturation limit. The rate constants at variable temperatures in Figure 3 predict that the step determining $^Dk_{cat}$ is unique from the one determining $^Dk_{cat}/K_M(O_2)$. According to a prior analysis of the mechanism in Scheme 3, $^Dk_{cat}$ reflects k_3,[21b] whereas $^Dk_{cat}/K_M(O_2)$ is derived from retention of the hydrogen abstracted from LA followed by peroxyl radical-mediated hydrogen atom abstraction from Y371 in k_7.[21c]

Preliminary results using Fe^{III}—COX-1 suggested $^Dk_{cat}$ to be >30 with h_{31}- and d_{31}-LA at 0.3 mM phenol.[13a] Although Wu et al.[22] have recently reported a much smaller $^Dk_{cat}$ value of ~2 for oxidation of selectively-labeled AA, their value is consistent with earlier estimates of the tritium KIE, $^Tk_{cat}/K_M(AA) \approx 4$.[20] It is common to observe inflated KIEs upon substitution of the native substrate by a weaker-binding analogue.[21b,c] In some cases, this is the result of unmasking the "chemical step", while in others, the identity of the rate-limiting step is unchanged and the KIE reflects the dependence of the tunneling probability on the hydrogen donor—acceptor distance. The modulation of this

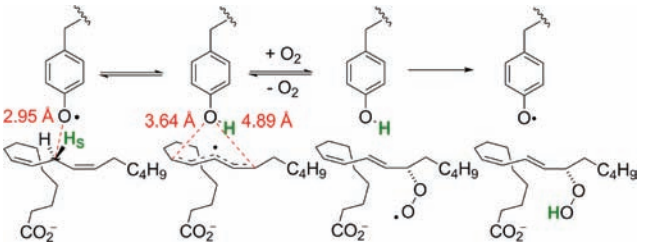

Figure 4. Proposed origin of $^Dk_{cat}/K_M(O_2)$. Heavy-atom distances are from the AA-bound structure in Figure 1.[11a]

Table 2. Rate Constants for Fe^{III}—COX-2 at 30 °C[a]

	h_{31}-LA		d_{31}-LA	
	k_{cat} (s^{-1})	$k_{cat}/K_M(O_2) \times 10^{-4}$ (M^{-1} s^{-1})	k_{cat} (s^{-1})	$k_{cat}/K_M(O_2) \times 10^{-3}$ (M^{-1} s^{-1})
H_2O	9.7 ± 0.6	4.0 ± 0.8	0.45 ± 0.02	6.5 ± 0.6
D_2O	4.3 ± 0.2	3.0 ± 0.4	0.43 ± 0.04	5.8 ± 0.8
SKIE[b]	2.3 ± 0.2	1.3 ± 0.3	0.94 ± 0.1	1.1 ± 0.2

[a] Derived from fitting to $V/[E]_T = k_{cat}[O_2]/(K_M + [O_2])$, with errors reported as $\pm 2\sigma_e$. [b] Apparent solvent kinetic isotope effect.

distance by protein motions over a range of time scales[23] may explain the anomalous temperature dependences.[24] Dynamical influences notwithstanding, AA is expected to exhibit a smaller KIE than LA because of its optimal positioning and contraction of the hydrogen donor—acceptor distance; this results in more comparable Franck—Condon overlap factors for H and D transfer.[21b]

Table 1 summarizes the KIEs obtained for LA oxidation at saturating and subsaturating concentrations of O_2, representing the nonphysiological and physiological ranges, respectively. The temperature independence of $^Dk_{cat}$ is consistent with LA binding in an optimal configuration and negligible thermal activation needed for C—H(D) homolysis. The significant isotope-independent activation energy (E_a = 9.14 ± 0.66 kcal mol^{-1}) derives from inner- and outer-sphere reorganization as well as the reaction thermodynamics.[23] Contrarily, the temperature dependence of $^Dk_{cat}/K_M(O_2)$ indicates a large variation of E_a, from 7.3 (h_{31}-LA) to 12.3 (d_{31}-LA) kcal mol^{-1}, due to thermally activated tunneling during O—H(D) homolysis.

Interestingly, the deuterium KIE on $k_{cat}/K_M(O_2)$ originates from the hydrogen isotope retained from LA. Such behavior has been observed in a related Y·-utilizing fatty acid dioxygenase.[21c] In the present study, the $^Dk_{cat}/K_M(O_2)$ value of 6.2 ± 1.6 derives from a large difference in isotopic activation energy [i.e., $E_a(D) - E_a(H)$ = 5.0 ± 0.78 kcal mol^{-1}, which exceeds the zero-point energy splitting] and an inverse A_H/A_D. These are indicators of thermally modulated tunneling[23a,24] where the isotope sensitivity of the activation barrier is attributed to the large-scale rearrangement needed to transfer the hydrogen from the O—H(D) of Y371 to the (9*R*)- or (13*S*)-peroxyl radical intermediate, regenerating the Y371· and forming the HPOD products (Figure 4).

The substrate deuterium KIE on Y371 reoxidation indicates solvent exchange that is slow on the time scale of enzyme turnover. The nearly indistinguishable values of $k_{cat}/K_M(O_2)$ with h_{31}-LA in H_2O and D_2O support this interpretation. A solvent KIE on k_{cat} is present for h_{31}-LA under these conditions, where

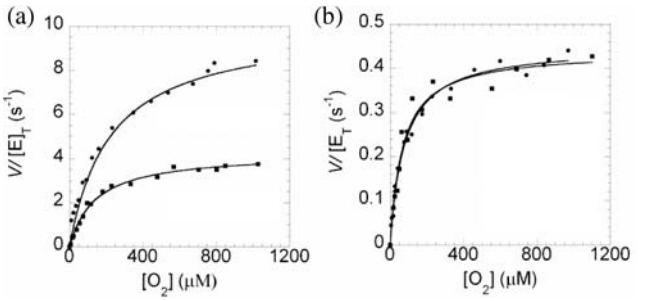

Figure 5. Steady-state kinetics of the oxidation of (a) h_{31}-LA and (b) d_{31}-LA (100 μM) by Fe^{III}−COX-2 in H_2O (●) and D_2O (■). Data were collected in the presence of 2 mM phenol at 30 °C.

the rate constants in Table 2 indicate $^{D_2O}k_{cat} = 2.3 \pm 0.2$. This effect vanishes when d_{31}-LA is used in place of h_{31}-LA because the diminution in k_{cat} masks the contribution from the solvent-exchangeable site. Substituting d_{31}-LA for h_{31}-LA also eliminates the very small $^{D_2O}k_{cat}/K_M(O_2)$, originating from $^{D_2O}k_{cat}$ and the offsetting influence of $^{D_2O}K_M(O_2)$, as shown in Figure 5.

We note that lipoxygenase (LOX) enzymes have structures disparate from COX, yet they react via similar controlled radical mechanisms.[1] Soybean LOX-1 oxidizes LA primarily to (13*S*)-HPOD,[25] whereas (9*R*)-HPOD is observed as the major product of COXs.[9] LOX-1 exhibits extensive nuclear tunneling with $^{D}k_{cat} \approx 80$ but no evidence of reversible C−H(D) homolysis.[19] In addition, $^{D}k_{cat}/K_M(O_2)$ has been difficult to establish. The present studies comparing AA to LA help to establish fundamental biochemical concepts as well as the relevance of LA in the larger field of oxidative biology, where COX and LOX colocalized within the mammalian cell compete for polyunsaturated fatty acids and O_2.

The findings from this study evidence multiple hydrogen tunneling steps during dioxygenase catalysis by human COX-2. Homolysis of the bisallylic C−H(D) in linoleic acid is largely rate-limiting at saturating levels of O_2, while O−H(D) homolysis of the reduced catalytic tyrosine becomes rate-limiting as the O_2 concentration is decreased to physiological levels. Importantly, the deuterium KIEs at 30 °C, $^{D}k_{cat} = 22$ and $^{D}k_{cat}/K_M(O_2) = 6.2$, are viewed as lower limits to possibly larger intrinsic values. The $^{D}k_{cat}$ is at least an order of magnitude greater than that determined with the native substrate, arachidonic acid, which reacts at a comparable rate. The inflated KIE with linoleic acid suggests an expanded hydrogen donor−acceptor distance, which diminishes the probability of D tunneling more than H tunneling. The temperature independence of $^{D}k_{cat}$ contrasts with the marked temperature dependence of $^{D}k_{cat}/K_M(O_2)$, signaling two hydrogen tunneling events characterized by unique activation parameters. These effects are observable because of slow solvent exchange with the precatalytic Y371 and the retention of the pro-*S* hydrogen from the isotopically labeled fatty acid substrates.

■ ASSOCIATED CONTENT

Supporting Information. Details of protein preparation and additional kinetic data. This material is available free of charge via the Internet at http://pubs.acs.org.

■ AUTHOR INFORMATION

Corresponding Author
jproth@jhu.edu.

■ ACKNOWLEDGMENT

We are grateful for support from NSF Grant MCB0919898 and assistance from Drs. Ah-Lim Tsai, Gang Wu, Mike Malkowski, Alex Vecchio, Kasia Rudzka, and Alfredo Angeles-Boza.

■ REFERENCES

(1) Rouzer, C. A.; Marnett, L. J. *Chem. Rev.* **2003**, *103*, 2239.
(2) Smith, W. L.; DeWitt, D. L.; Garavito, R. M. *Annu. Rev. Biochem.* **2000**, *69*, 145.
(3) Halliwell, B.; Gutteridge, J. M. C. *Free Radicals in Biology and Medicine*, 3rd Ed.; Oxford University Press: New York, 2005.
(4) Marnett, L. J. *Annu. Rev. Pharmacol. Toxicol.* **2009**, *49*, 265.
(5) Menter, D. G.; Schilsky, R. L.; DuBois, R. N. *Clin. Cancer Res.* **2010**, *16*, 1384.
(6) Tsai, A.-L.; Kulmacz, R. J. *Arch. Biochem. Biophys.* **2010**, *493*, 103.
(7) (a) van der Ouderaa, F. J.; Buytenhek, M.; Nugteren, D. H.; Van Dorp, D. A. *Biochim. Biophys. Acta* **1977**, *487*, 315. (b) Tsai, A.-L.; Hsi, L. C.; Kulmacz, R. J.; Palmer, G.; Smith, W. L. *J. Biol. Chem.* **1994**, *269*, 5085.
(8) Mukherjee, A.; Brinkley, D. W.; Chang, K. M.; Roth, J. P. *Biochemistry* **2007**, *46*, 3975.
(9) Hamberg, M. *Arch. Biochem. Biophys.* **1998**, *349*, 376.
(10) Malkowski, M. G.; Ginell, S. L.; Smith, W. L.; Garavito, R. M. *Science* **2000**, *289*, 1933.
(11) (a) Vecchio, A. J.; Simmons, D. M.; Malkowski, M. G. *J. Biol. Chem.* **2010**, *285*, 22152. (b) Dong, L.; Vecchio, A. J.; Sharma, N. P.; Jurban, B. J.; Malkowski, M. G.; Smith, W. L. *J. Biol. Chem.* **2011**, *286*, 19035.
(12) The KIEs were independent of the preparations of COX-2 as well as the h_{31}- and d_{31}-LA, which were stored at −30 °C under N_2. d_{31}-LA was used as received (Sigma/Isotech, >98%) or purified from an algal mixture following a published procedure (see: Lewis, E.; Johansen, E.; Holman, T. R. *J. Am. Chem. Soc.* **1999**, *121*, 1395).
(13) (a) Mukherjee, A. Ph.D. Dissertation, Johns Hopkins University, Baltimore, MD, 2009. (b) See the Supporting Information for details.
(14) Hsuanyu, Y.; Dunford, H. B. *J. Biol. Chem.* **1992**, *267*, 17649.
(15) Wu, G.; Tsai, A.-L.; Kulmacz, R. J. *Biochemistry* **2009**, *48*, 11902.
(16) Kulmacz, R. J.; van der Donk, W. A.; Tsai, A.-L. *Prog. Lipid Res.* **2003**, *42*, 377.
(17) Yuan, C.; Rieke, C. J.; Rimon, G.; Wingerd, B. A.; Smith, W. L. *Proc. Natl. Acad. Sci. U.S.A.* **2006**, *103*, 6142.
(18) Goodwin, D. C.; Rowlinson, S. W.; Marnett, L. J. *Biochemistry* **2000**, *39*, 5422. The following extinction coefficients are given per monomer: $\varepsilon_{407} = 129\,000\ M^{-1}\ cm^{-1}$ for Fe^{III}−COX-2 and $\varepsilon_{375} = 66\,000\ M^{-1}\ cm^{-1}$ and $\varepsilon_{470} = 42\,000\ M^{-1}\ cm^{-1}$ for Mn^{III}−COX-2.
(19) Glickman, M. H.; Klinman, J. P. *Biochemistry* **1995**, *34*, 14077.
(20) (a) Hamberg, M.; Samuelsson, B. *J. Biol. Chem.* **1967**, *242*, 5336. (b) Schneider, C.; Brash, A. R. *J. Biol. Chem.* **2000**, *275*, 4743.
(21) (a) Gupta, A.; Mukherjee, A.; Matsui, K.; Roth, J. P. *J. Am. Chem. Soc.* **2008**, *130*, 11274. (b) Mukherjee, A.; Angeles-Boza, A. M.; Huff, G. S.; Roth, J. P. *J. Am. Chem. Soc.* **2011**, *133*, 227. (c) Huff, G. S.; Doncheva, I. D.; Brinkley, D. W.; Angeles-Boza, A. M.; Mukherjee, A.; Cramer, C. J.; Roth, J. P. *Biochemistry* **2011**, *50*, 7375.
(22) Wu, G.; Lü, J.-M.; van der Donk, W. A.; Kulmacz, R. J.; Tsai, A.-L. *J. Inorg. Biochem.* **2011**, *105*, 382.
(23) (a) Nagel, Z, D.; Klinman, J. P. *Nat. Chem. Biol.* **2009**, *5*, 543. (b) Hammes-Schiffer, S. *Acc. Chem. Res.* **2006**, *39*, 93.
(24) (a) Schwartz, S. D; Schramm, V. L. *Nat. Chem. Biol.* **2009**, *5*, 551. (b) Johannissen, L. O.; Scrutton, N. S.; Sutcliffe, M. J. *Angew. Chem., Int. Ed.* **2011**, *50*, 2129.
(25) Knapp, M. J.; Seebeck, F. P.; Klinman, J. P. *J. Am. Chem. Soc.* **2001**, *123*, 2931.